JOURNAL OF MATERIALS SCIENCE 26 (1991) 1699–1704

Surface nucleation and cellular growth kinetics of cordierite glass ceramics containing 3 mol % Y_2O_3–ZrO_2

YUAN-JANG SUE, SAN-YUAN CHEN*, HONG-YANG LU, POUYAN SHEN
Institute of Materials Science and Engineering, National Sun Yat-Sen University, Kaohsiung 80424, Taiwan
**Materials Research Laboratories, Industrial Technology Research Institute, Chutung 31015, Taiwan*

Cordierite-based glass ceramics of the $2MgO:2Al_2O_3:5SiO_2$ composition with t-ZrO_2 (3 mol % Y_2O_3–ZrO_2) and P_2O_5 addition, was heat-treated isothermally and isochronically for crystallization studies. Major crystalline phases incurred by the heat treatment were t-ZrO_2 and α-cordierite. Surface nucleation predominated when edge and corner nucleation in these samples were suppressed regardless of their radii of curvature. Crystallization began with the formation of β-quartz s.s. and its transformation to α-cordierite was followed by prolonged heating. Cellular growth of α-cordierite on the surface of the quenched glass plates, gave a linear kinetics. The activation energy for cellular growth was ~ 410 kJ mol^{-1}.

1. Introduction

Cordierite-based glass ceramics have been widely utilized for their low thermal expansion coefficients and good thermal shock resistance [1, 2]. It is commonly processed by a heat-treatment of the cordierite composition glass in one or two steps at temperatures ranging from 800 to 1300 °C [1–7]. Additives such as ZrO_2, TiO_2, P_2O_5 among other alkali oxides [1, 8] were used in processing these glass ceramics to promote the nucleation. Apart from acting as a nucleation agent, ZrO_2 has also been demonstrated to improve the fracture toughness of cordierite as well as other glass ceramics [9–12].

The devitrification of ZrO_2-added cordierite glass ceramics involved the following steps: (1) liquid phase separation to form a ZrO_2-rich droplet and SiO_2-rich matrix [13]; (2) crystallization of a metastable but dominant β-quartz s.s., ZrO_2, Al-Mg spinel and cristobalite [14]; (3) transformation of β-quartz s.s. to μ-cordierite and then to α-cordierite [15]. It was generally believed that the transition between β-quartz and μ-cordierite involved composition variation [4, 14], whereas μ-cordierite and α-cordierite were two of the known three polymorphs [5, 16] with α-cordierite being the stable phase. Heat treatment of the sintered cordierite composition glass powder discs [6, 11, 17] resulted in a different microstructure from that of the quenched glass plates [18, 19], although surface nucleation was involved in both cases. In contrast to the fine grain size cordierite and ZrO_2 in viscous sintered samples [11], the heat-treated glass plate has dendrites formed by cellular growth on the surface layer [17–19] and spherulite in the interior. Segregation of ZrO_2 at grain boundaries [20, 21] as well as preferentially along the crystallographic directions of cordierite [7, 21] was also observed. Phase separation prior to crystallization [21] was found in 3 mol % Y_2O_3–ZrO_2 added cordierite glass ceramics. Partition of Y_2O_3 between ZrO_2 and glass was also suggested in a recent study of the Y_2O_3–Al_2O_3–SiO_2 glass system [22]. It would be interesting to study how the crystallization kinetics are affected by the phase separation and the partition effect.

Recently, Chen and King [23] has shown that diffusion induced recrystallization (DIR) occurs along edges and at the corners of the copper single-crystal specimen. They also found that edge nucleation is suppressed when the radius of curvature of the edges is increased to approximately 40 μm. It is not known if edge nucleation is also affected by the radius of curvature in glass ceramics.

Crystallization kinetics of 3 mol % Y_2O_3–ZrO_2 added cordierite glass composition was therefore investigated in the present study. Activation energy and crystallization temperature in the cordierite composition glass ceramics were determined and the effect of curvature of edge on nucleation was discussed.

2. Experimental procedures

Quenched glass plates of the composition of stoichiometric cordierite with 3 wt % P_2O_5, 5 wt % 3 mol % Y_2O_3–ZrO_2 additions were heat treated at 950 to 1420 °C for 0.5 to 75 h. P_2O_5 was added to assist the crystallization [24]. Glass plates sectioned by using a diamond-embedded saw, were polished successively by using γ-Al_2O_3 powder to samples of final dimensions of ~ 1 × 1 × 1 cm^3 and ~ 0.5 × 0.5 × 0.5 cm^3.

0022–2461/91 $03.00 + .12

TABLE II Optical microscopy observations of crystalline phases and microstructural development in devitrified glass plates

Treatment	T(°C)	t(min)	Surface layer	W(μm)	L(mm)	Interior	$V(t)$[a]
Isochronical for 5 h	950	–	β-quartz s.s. in glass	5	N.D	glass	–
	1000	–	β-quartz and α-cordierite	10	0.17	glass	–
	1050	–	α-cordierite	29	0.44	glass	–
	1100	–	α-cordierite (with domains)	52	2	α-cordierite with domains	–
	1150	–	as above	66	5	as above	–
	1200	–	as above	104	12	as above	–
Isochronical for 0.5 h	1250	–	α-cordierite (with domain)	24	1.5	α-cordierite with domains	–
	1300	–	α-cordierite and glass	23	1.5	spherulitic α-cordierite	–
	1370	–	as above	18	0.9	as above	–
	1420	–	as above	15	0.8	as above	–
Isothermal at 1000 °C		180	cellular β-quartz s.s and α-cordierite	–	–	glass	10 ± 4%
		420	as above	–	–	glass	17 ± 5%
		540	cellullar α-cordierite	–	–	spherulitic α-cordierite in glass	38 ± 6%
		670	as above	–	–	as above	50 ± 5%
		1080	as above	–	–	as above	71 ± 5%
		1500	as above	–	–	as above	87 ± 7%
		3000	as above	–	–	recrystallized α-cordierite	~ 100%

[a] $V(t)$ represented crystallinity determined by XRD.
W and L: dimensions of cellular crystal measured perpendicular and parallel to the cellular growth direction.
Note: (a) identification of crystalline phases were also confirmed by XRD;
(b) minor t-ZrO_2 was present in both surface and internal nucleated region (see text).

α-cordierite started to appear in samples treated at 1000 °C together with the disappearance of β-quartz s.s.. Mullite also was found to accompany with α-cordierite and t-ZrO_2 for samples treated at > 1300 °C for 0.5 h. When isothermally treated at 1000 °C for more than 3 h (Table II), and up to 50 h, there was no β-quartz s.s. and only α-cordierite was found.

3.3. DTA analysis

The principal features shown by the DTA results of glass plate compositions (Fig. 3) were the glass transition (T_g ~ 837 °C), the shallow endotherm corresponding to the M_g range (M_g ~ 850 °C) [4, 29], the initial crystallization (~ 924 °C), and the conversion to α-cordierite (1005 °C). The two exothermic peaks at 924 and 1005 °C corresponded to the crystallization temperature of β-quartz s.s. and t-ZrO_2, and the transition temperature of β-quartz s.s. to α-cordierite.

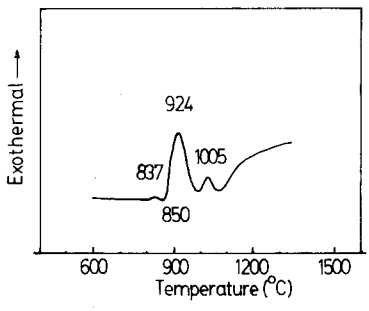

Figure 3 DTA curve of glass plate.

3.4. Cellular growth of α-cordierite

The microstructure of glass plates heat-treated at various temperatures were compiled in Table II. The cellular crystals of α-cordierite were firstly formed at the surface (Fig. 4) and the subsequent growth proceeded inwards. The crystal orientation of α-cordierite from the adjacent surfaces changed abruptly thus forming interfaces (as indicated in Fig. 4). The acute edge had only one interface (Fig. 4a); whereas the corner with obtuse angle resulted in two interfaces (Fig. 4b). The latter appeared in three sections of α-cordierite having different crystal orientations (Fig. 4b). The indication therefore was that surface nucleation rather than edge or corner nucleation dominated during the crystallization of cellular α-cordierite.

Growth rate as measured by optical polarized microscope indicated that the length of cellular crystals increased linearly with isothermal heat-treatment duration. The cellular growth rate was almost tripled from 0.56 mm min^{-1} at 1000 °C to 1.48 mm min^{-1} at 1050 °C (Fig. 5). Cellular lengths resulted from isochronical heat treatment at various temperatures (Table II) were also measured to construct the growth rate against ($1/T$) plot (Fig. 6). Estimation of the activation energy by plotting Arrhenius relation gave ~ 410 kJ mol^{-1} for the cellular α-cordierite growth in quenched glass plates, as shown in Fig. 7. It indicated that the cellular growth of α-cordierite was controlled by the same mechanism in the temperature range studied. The growth rate of cellular α-cordierite crystals reached maximum at ~1250 to 1300 °C (Table II).

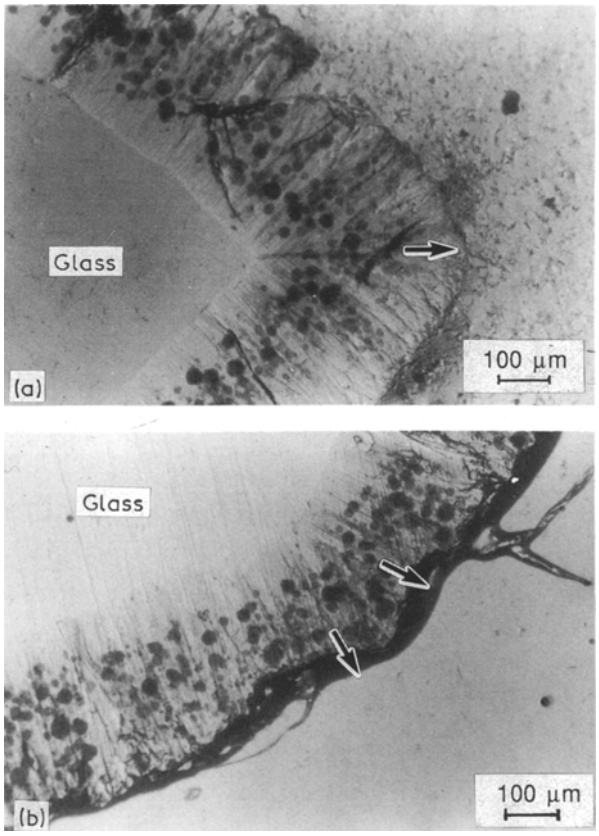

Figure 4 Optical micrographs (open nicol) showing cellular growth (950 °C, 25 h) at (a) acute edge, and (b) obtuse edge. The arrows indicate the interfaces of cellular crystals nucleated and grown from adjacent surfaces.

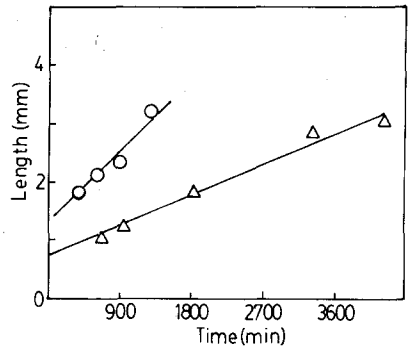

Figure 5 Length of cellular cordierite crystals in glass plates fired at 1050 °C (○) and 1000 °C (△).

4. Discussion

4.1. Nucleation

The crystallization of α-cordierite started from surface inwards (Fig. 4) and the very different crystal morphology betweeen the interior and the surface [21], implied that surface nucleation and internal nucleation [7] concurrently occurred during heat treatment. Similar to copper single crystal [23], edge nucleation appeared to have been suppressed, and it also appeared that regardless of the shape of sample corners, either acute or obtuse, surface nucleation predominated over edge and corner nucleation. Although the crystals nucleating at surfaces may be randomly oriented [30], the crystals oriented with the fast growth direction perpendicular to the surface took precedence. Hence the α-cordierite crystals being surface-nucleated, grew perpendicularly to the surface until meeting with the adjacent crystals.

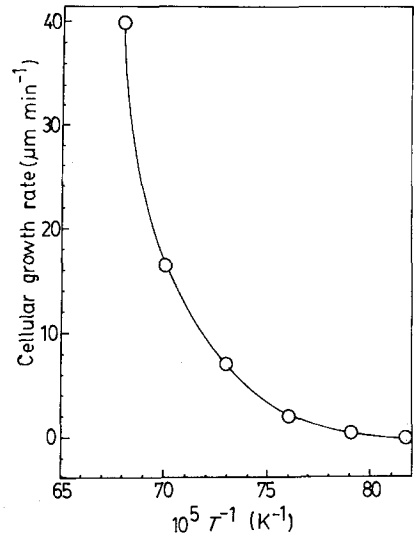

Figure 6 Cellular growth rate against $1/T$ plot.

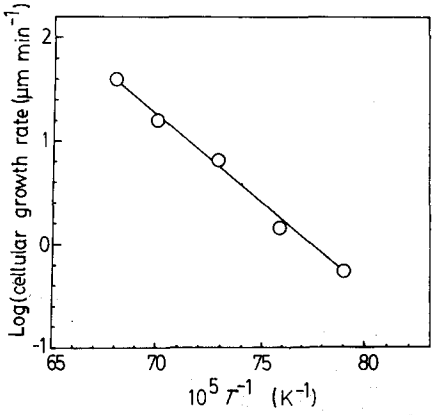

Figure 7 Arrhenius plot of logarithmic cellular growth rate as a function of $1/T$. $E_a = 410\ \mathrm{kJ\,mol^{-1}}$.

4.2. Crystallization kinetics

The n number of the JMA plots (Fig. 2) were 1.47 and 0.46 for samples heat treated at 1000 and 1050 °C. Growth kinetics from the present study were different from the results of an interface-controlled linear growth kinetics obtained in a 15 wt % ZrO_2–added cordierite composition glass [7]. The linear kinetics [7] resulted from the cellular growth of α-cordierite indicated an interface-controlled mechanism, and redistribution of ZrO_2 could be responsible for the rate-controlling [7]. Adopting the spherulite growth theory in polymer [19, 31], however, an interface-controlled mechanism was represented [31] by $n = 3$. Since both cellular, spherulitic growth and ZrO_2 segregation occurred in the present sample, the interpretation of n number in terms of crystal morphology was not attempted.

The combination of homogeneous–heterogeneous nucleation [31] may account in part for the crystallization kinetics of non-integer n number. And only samples heat-treated at 1000 °C ($n = 1.47$) fitted in

the typical number of between 1 and 2 [33] for oxide glass systems such as Li_2–SiO_2, BaO–SiO_2 and Na_2O–P_2O_5, where a combination of homogeneous–heterogeneous nucleation may have occurred. Due to the fact that many crystalline phases have emerged, the kinetics observed were also a combination of the crystallization of β-quartz s.s., t-ZrO_2 and α-cordierite (Table I), and the phase transition of β-quartz s.s. to α-cordierite occurred at $\sim 1005\,^{\circ}C$ (Fig. 3).

4.3. Activation energy of cellular growth

Activation energy (E_a) of $\sim 272\,kJ\,mol^{-1}$ [29] for the crystallization of cordierite-composition glass powder discs, was much less than the E_a $\sim 410\,kJ\,mol^{-1}$ estimated in this study. Composition affecting the viscosity was taken to account for the discrepancy obtained in the activation energy [29]. It can probably be taken to explain the present difference in the E_a by the t-ZrO_2 content and the presence of Y_2O_3 in the glass composition. Phase separation [21] and the partition of yttria between ZrO_2 and glass [23] would also affect the viscosity of the glass upon crystallization. Alternatively, the control mechanism in the crystallization of cordierite in quenched plates may be different from that in sintered glass powder compact.

4.4. Catalysed crystallization

The catalysed crystallization generally involved two processes: (1) the control of phase separation in glass, and (2) the direct deposition of substance (epitaxy) on the crystal nuclei [34]. The observation of colloidal ZrO_2-rich droplets formed by glass-in-glass phase separation [21] has, in fact, indicated that nucleation and subsequent growth would be different from what was reported in the cordierite composition glass powder without ZrO_2 [29]. ZrO_2 having a definite solubility in the cordierite composition glass [19] forming ZrO_4-tetrahedra when dissolved, would act as a nucleating catalyst [3] which promoted the heterogeneous nucleation and therefore increased the nucleation rate. Two mechanisms involving t-ZrO_2 were possible.

(1) Homogeneous nucleation: ZrO_2-enriched phase was formed firstly during glass-in-glass phase separation, then β-quartz s.s. formed, and which transformed to α-cordierite before t-ZrO_2 was expelled to grain boundaries [21].

(2) Heterogeneous nucleation: precipitation of t-ZrO_2 provided the epitaxial growth of β-quartz s.s., which transformed to α-cordierite, then the t-ZrO_2 was expelled to grain boundaries [21].

5. Conclusions

The following conclusions may be drawn from crystallization of cordierite–3 mol % Y_2O_3–ZrO_2 glass plate:

(1) The crystallization kinetics can be fitted to the JMA theory with the n value of 0.46 and 1.47 for devitrification at 1050 and 1000 °C, respectively.

(2) Nucleation occurred from sample surface, rather than from edge or corner, and grew inwards. The crystal orientation of α-cordierite from the adjacent surfaces changed abruptly and then formed interfaces.

(3) Cellular growth of α-cordierite on the surface of quenched glass plates resulted in a linear kinetics and was interface controlled.

(4) The activation energy for the cellular growth was $\sim 410\,kJ\,mol^{-1}$.

Acknowledgements

Thanks are due to Mr Wen-Hsiung Hsu of Union Chemical Labs., Industrial Technology Research Institute for assisting prepare the glass plates.

References

1. P. W. McMILLAN, "Glass Ceramics," 2nd Edn (Academic, New York, 1979) p. 225.
2. T. MATSUHISA and S. SOEJIMA, US Patent 4,280,845 (1981).
3. W. VOGEL and W. HOLAND, "Advances in Ceramics," Vol. 4, edited by J. H. Simmon, D. R. Uhlmann and G. H. Beall (American Ceramic Society, Columbus OH, 1982).
4. W. ZDANIEWSKI, *J. Amer. Ceram. Soc.* **58** (1975) 163.
5. M. D. KARKHANAVALA and F. A. HUMMEL, *ibid.* **36** (1953) 389.
6. E. A. GIESS, J. P. FLETCHER and L. W. HERRON, *ibid.* **67** (1984) 549.
7. M. A. McCOY, W. E. LEE and A. H. HEUER, *ibid.* **69** (1986) 292.
8. A. G. GREGORY and T. J. VEASEY, *J. Mater. Sci.* **8** (1973) 324.
9. M. NOGAMI and M. TOMOZAWA, *J. Amer. Ceram. Soc.* **69** (1986) 99.
10. Y. SHEN and R. J. BROOK, *Ceram. Int.* **9** (1983) 39.
11. B. H. MUSSLER and M. W. SHAFER, *Amer. Ceram. Soc. Bull.* **64** (1985) 1459.
12. M. A. McCOY and A. H. HEUER, *J. Amer. Ceram. Soc.* **71** (1988) 673.
13. G. F. NEILSON, *J. Appl. Phys.* **43** (1972) 3728.
14. T. I. BARRY, J. M. COX and R. MORRELL, *J. Mater. Sci.* **13** (1978) 594.
15. K. LANGER and W. SCHREYER, *Am. Mineral.* **54** (1969) 1442.
16. E. P. MEAGHER and G. V. GIBBS, *Can. Mineral.* **15** (1977) 43.
17. E. M. RABINOVICH, in "Advances in Ceramics," Vol. 4, edited by J. H. Simmons, D. R. Uhlmann and G. H. Bell (*American Ceramic. Society*, Columbus OH, 1982) pp. 327–333.
18. K. WATANABE, E. A. GIESS and M. W. SHAFER, *J. Mater. Sci.* **20** (1985) 508.
19. W. A. ZDANIEWSKI, *J. Amer. Ceram. Soc.* **61** (1978) 199.
20. T. DUMAS, A. RAMOS. M. GANDAIS and J. PETIAU, *J. Mater. Sci. Lett.* **4** (1985) 129.
21. Y. J. SUE, P. SHEN, S. Y. CHEN and H. Y. LU, *J. Amer. Ceram. Soc.* in press.
22. Y. CHENG and D. P. THOMPSON, *Brit. Ceram. Trans. J.* **87** (1988) 107.
23. F. S. CHEN and A. H. KING, *Scripta Metall.* **21** (1987) 649.
24. P. W. McMILLAN, "Glass Ceramics", 2nd Edn (Academic, New York, 1979) p. 95.
25. S. M. OHLBERG and D. W. STRICKLER, *J. Amer. Ceram. Soc.* **45** (1962) 170.
26. W. A. JOHNSON and R. F. MEHL, *Trans. Metall. Soc. AIME* **135** (1939) 416.
27. A. AVRAMI, *J. Chem. Phys.* **7** (1939) 103.
28. *Idem., ibid.* **8** (1940) 212.
29. K. WATANABE and E. A. GIESS, *J. Amer. Ceram. Soc.* **68** (1985) C102.
30. M. H. LEWIS, J. METCALF-JOHANSEN and P. S. BELL, *ibid.* **62** (1979) 278.

31. D. C. BASSET, "Principles of Polymer Morphology" (Cambridge University Press, Cambridge, UK, 1981) p. 165.
32. W. VOGEL, "Chemistry of Glass" (American Ceramic Society, Columbus OH, 1985) p. 223.
33. P. W. McMILLAN, "Glass Ceramics", 2nd Edn (Academic, New York, 1979) p. 57.
34. W. VOGEL and K. GERTH, "Catalyzed Crystallization in Glasses", in Symposium on Nucleation and Crystallization in Glasses and Melts (American Ceramic Society, Columbus OH, 1962).

Received 17 October 1989
and accepted 20 March 1990